A Pulsed Ion Deflection System for Background Reduction in ^{252}Cf-Plasma Desorption Mass Spectrometry

Barbara Wolf and Ronald D. Macfarlane
Department of Chemistry, Texas A&M University, College Station, Texas, USA

The use of an electrostatic particle guide (EPG) for background reduction in a time-of-flight mass spectrometer is described. Operating with reverse polarity, the EPG deflects ions radially from the beam axis, separating the ionic and neutral components of the beam. Use of the deflection EPG in a synchronized pulsed mode with a barrier disk aligned in the center of the beam axis eliminates up to 80% of the spectral background in the molecular ion region of an insulin spectrum obtained by ^{252}Cf-plasma desorption mass spectrometry. The background eliminated is due to the neutral products of metastable fragmentation and to uncorrelated events. Although peak intensities are reduced when the pulsed deflection EPG system is used, the reduction in background achieved is greater, resulting in an overall improvement in peak-to-background ratios of up to a factor of three. A new large-area stop detector designed for use with the pulsed deflection EPG is described. The new hybrid detector, which utilizes the combination of a large (75-mm active diameter) microchannel plate (MCP) and a scintillation detector, provides greater sensitivity for high-mass ions than a conventional MCP chevron detector. *(J Am Soc Mass Spectrom 1992, 3, 706–715)*

The method of ^{252}Cf-plasma desorption mass spectrometry (PDMS) is routinely used in many laboratories to analyze proteins of molecular weights up to m/z 25,000 [1]. The current mass range capability of ^{252}Cf-PDMS for proteins has been established at m/z 45,000 with the observation of the ovalbumin molecular ion [2] and for metal cluster ions at m/z 105,000 [3]. Recently, two mass spectrometric methods, matrix-assisted laser desorption [4] and electrospray ionization [5], were used to detect proteins having molecular weights beyond 100,000. Currently, one of the problems influencing the performance of ^{252}Cf-PDMS for high mass ions is the relatively low peak-to-background ratio in the high mass region.

In ^{252}Cf-PDMS, an event that contributes to the time-of-flight (TOF) spectrum is recorded when the ion detector at the end of the flight tube (stop detector) generates an electronic pulse while the time-to-digital converter is activated. The pulse can be initiated by a fast particle hitting the detector or by the spontaneous firing of the electron multiplier without particles hitting the detector. This event is called electronic noise. In a single-ion counting technique such as ^{252}Cf-PDMS, electronic noise is negligible. The background in PDMS is composed primarily of products of metastable fragmentation and uncorrelated events. Sundqvist et al. [6] estimate that the neutral products of metastable decay contribute approximately 20% to a typical PDMS spectrum. The majority of the smooth background continuum observed in PDMS spectra is due to the detection of ions that are not correlated in time with the desorption event (uncorrelated events) [7]. When a ^{252}Cf fission fragment passes through the sample foil, a start pulse is generated by detecting the complementary fission fragment. The start pulse is fed into a time interval digitizer (TID) that opens a time window of specifiable length during which any number of stop pulses are accepted. During the time window, no new start pulses are accepted by the TID. Because ^{252}Cf fission fragments impinge on the sample at a rate on the order of 1000/s, the time separation between actual start pulses is on the order of 1 ms. The time window selected for the TID is dependent on the flight path length and acceleration voltage, as well as the mass of the protein to be analyzed. Typically, time windows are on the order of tens of microseconds. Thus, the probability for a second start event to occur within the time window is on the order of a few percent. Sample ions desorbed by the second start event will be detected and, because they are not correlated in time with the spectrum being collected, contribute to the background continuum.

One approach to increasing the high mass detection limit is to lower the spectral background. A high background in a ^{252}Cf-PDMS spectrum adversely af-

Address reprint requests to Ronald D. Macfarlane, Department of Chemistry, Texas A&M University, College Station, TX 77845.

1044–0305/92/$5.00

Received November 25, 1991
Revised March 6, 1992
Accepted March 6, 1992

fects the sensitivity for detecting weak intensity peaks in the spectrum. Because the background has a statistical origin, the level fluctuates from one data point to another, and the amplitude of the fluctuation is approximately the square root of N for each data point, where N is the number of events in a particular channel. For example, if a particular channel has accumulated 10,000 events, the uncertainty in that value is 100 or 1%. If, in that region, a true peak is present, but with a peak intensity of 50 events above the background, it is lost in the statistical fluctuation of the background. If the background is then reduced to 100 events, the statistical fluctuation is on the order of 10 events/channel and the 50 events from the weak (but real) peak are now statistically significant and discernible.

We previously introduced the use of an electrostatic particle guide (EPG) as an ion deflection device for the purpose of separating the neutral component of a PDMS spectrum from the ion component [8]. EPGs are conventionally used to minimize beam divergence by trapping ions in a spiral trajectory [9]. The device operates by injecting an ion into an electric field generated by two concentric cylinders. The inner cylinder is a thin wire aligned with the beam axis and held at a potential that is attractive for the injected ion. Depending on the angle of incidence of the ion into the particle guide, the ion traverses the tube while spiraling around the central wire. If the ion enters the particle guide with a trajectory that is exactly parallel to the central wire, it has no relative angular momentum and the ion takes on a collision course with the wire. When used as an ion deflector, the potential placed on the inner electrode is repulsive to the injected ions. Ions are deflected radially from the center wire, resulting in the formation of an annular beam of ions separated from the unperturbed neutral component. By deflecting ions out of range of detection, we were able to study the neutral component of spectra. In addition, we employed a synchronized pulsed deflection to reduce the magnitude of uncorrelated background in PDMS spectra. In that application the deflection voltage was applied continuously, but was pulsed off for a time interval corresponding to the period during which ions of interest traversed the EPG.

In this article we present an alternative pulsed deflection technique that provides a dramatic reduction in background and an improvement in the peak-to-background ratio for high mass ions, far superior to that obtainable using the pulsed off method.

Experimental

Instrumentation

The ^{252}Cf-PDMS configuration used for this study is depicted in Figure 1. In this linear PDMS system the ^{252}Cf source was located 5 mm from the start detector and 2 mm from the sample target. The acceleration

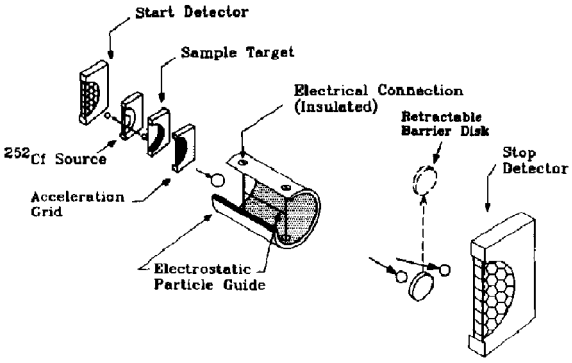

Figure 1. Isometric cutaway view of the ^{252}Cf-PDMS spectrometer, including the deflection EPG and barrier disk.

grid was 8 mm from the sample target and the EPG was positioned 28 mm downstream from the grid. The outer conductor of the EPG was a stainless steel cylinder, 12.8 cm long, 3 mm thick, with a 2.3-cm inside diameter. The inner conductor was a 1.6-mm-diameter stainless steel rod 14 cm in length. The rigid rod was used as the inner conductor to circumvent the difficulty encountered in mounting a uniformly linear wire with minimal field inhomogeneities. The rod was supported at one end of the EPG by a thin (0.635-mm) stainless steel plate that fitted into a slot in the outer cylinder. The plate and rod were electrically insulated from the outer cylinder by Delrin inserts so that voltage could be applied to the rod while the outer cylinder remained at ground potential.

A retractable barrier disk was positioned 70 mm in front of the stop detector, 35.4 cm downstream of the EPG. The disk was mounted on a push–pull type high vacuum feedthrough (Huntington Laboratories, Inc., Mountain View, CA) having 60-mm travel, such that the disk could be placed in the center of the beam axis or retracted completely out of ion range. The selection of the diameter of the barrier disk, 38 mm, was determined in part by computer simulation and also by experimental trial and error. The start detector consisted of two 18-mm active diameter microchannel plates (Galileo Electro-Optics, Galileo Park, Sturbridge, MA) in a chevron configuration and a large (25-mm diameter) conversion foil of 1.5-μm aluminized Mylar.

Stop detector. To increase the gain of the stop detector and to increase the detector area for use with the deflection EPG, we developed a new hybrid design in which a large area microchannel plate (MCP) is coupled with a scintillation detector. Ions impinge on the single, 75-mm active diameter MCP, providing 10^3 gain. The electrons emitted from the MCP are electrostatically focused onto a scintillator coupled to a fast timing photomultiplier tube that provides an additional 10^6 gain. The higher total gain (10^9) increases the signal-to-noise ratio for the small-amplitude pulses produced by high-mass ions. An electrostatics simula-

tion program, SIMION [10], was used to assist in the design of the detector. The design criterion required that electrons be accelerated and focused onto the 25-mm diameter scintillator from the 75-mm diameter MCP. The SIMION plot in Figure 2 shows the trajectories of electrons between the MCP and the scintillator in the selected design. As shown, the stainless steel focusing ring is 20 mm long with an inside diameter of 79 mm. The ring is positioned 6 mm from the MCP. The distance between the MCP and the scintillator is 96 mm. The back side of the MCP and the focusing ring are both at ground potential, and the grid (90% transmission nickel mesh) positioned in front of the scintillator is held at +5 kV. The front side of the MCP is held at −1 kV to provide the 1-kV potential drop across the MCP that is required for operation. The scintillator used was a 25-mm diameter, 1-mm-thick disk of polystyrene doped with a fluorescent molecule (BC-404, Bicron Corp., Newbury, OH). The rise time associated with scintillation was 0.7 ns. The scintillator wafer was coupled to the photomultiplier tube (PMT) by a 40-mm long Pyrex light guide, 25 mm in diameter. The light guide was cemented with high-vacuum cement to a Vac-U-Flat flange (Huntington Laboratories, Inc.) so that it could be easily attached to the high vacuum chamber (10^{-7} torr) containing the ^{252}Cf-PDMS spectrometer. The PMT selected was model R3082 from Hamamatsu Corporation (Bridgewater, NJ). The PMT was a 25-mm-diameter head-on type tube with a linear dynode structure having 10 stages and a rise time of 2 ns.

Principles and Simulations

The EPG is operated as an ion deflection device by placing a voltage on the inner electrode of the EPG that is of the same polarity as that of the accelerated ions passing through it. The outer electrode is held at ground potential, and the resulting electric field within the EPG increases the radial component of velocity of the ions. If the equipotential field lines are parallel to the beam axis, the axial component of the ions' velocity is not perturbed, with the result that the TOF of ions is not affected by the action of the EPG. However, the fringe electrostatic fields at the ends of the EPG can significantly perturb an ion's axial velocity and hence its TOF value [11].

The radial deflection of ions by the EPG results in the formation of an annular beam of ions that is separated from the neutral products of metastable ion decay that continue to travel parallel to the spectrometer axis. By positioning the barrier disk in the center of the spectrometer axis (Figure 1), the major part of the neutral component of the spectrum can be blocked before reaching the ion detector. An optimum deflection voltage must be selected to allow the maximum number of ions to reach the detector. For this purpose the simulation program SIMION was used to model the deflection system at various EPG voltages. A plot of the SIMION calculated trajectories for the optimum deflection voltage (+70 V) for positive ions (with an energy of +15 keV) is shown in Figure 3. This voltage provided enough deflection that ions were not blocked by the barrier disk, but not so much deflection that they were deflected beyond the range of the detector. The ion trajectories shown were calculated for ions of m/z 1; however, the radial distance traveled by ions with the same entrance angle as a result of the EPG deflection is independent of mass. In the simulation, the ions were emitted with an initial kinetic energy of 3 eV [12] and normal to a 20-mm^2 target area. Use of the deflection EPG with the barrier disk can virtually eliminate the neutral component of background from a ^{252}Cf-PDMS spectrum.

The next phase of development of the deflection EPG was to use it in a pulsed mode as an electrostatic gate. The general procedure is the following. With the barrier disk in position, the deflection EPG is turned on for a gated period to deflect selected ions past the barrier disk. If the approximate mass of the ion of interest is known or determined from a short acquisition without the deflection EPG, then one can calculate the time at which the ion enters and exits the EPG. A pulser circuit is then set up to turn the deflection voltage on only during the time period that the ion is inside the EPG. Because the deflection voltage is off before and after this time period, all ions that are not located within the EPG during the deflection period

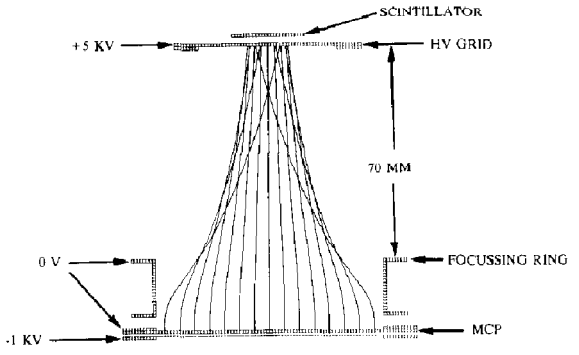

Figure 2. SIMION plot of a region of the hybrid stop detector showing simulated trajectories of electrons traveling from the back side of the MCP to the scintillator.

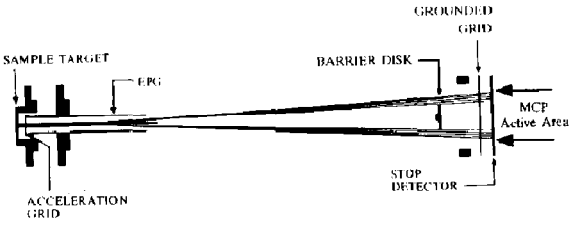

Figure 3. SIMION calculated trajectories for +70 V on the deflection EPG. The active area of the stop detector MCP is located in the region between the arrows.

strike the barrier disk. In addition, all neutrals strike the barrier disk. In this way, not only the neutral species background, but also much of the background due to uncorrelated events is eliminated from the ^{252}Cf-PDMS spectrum.

The pulser used in these experiments was a high-voltage pulser (model HV1000-P, Directed Energy, Inc., Fort Collins, CO) capable of pulsing voltages up to +900 V. A block diagram of the pulser circuitry is shown in Figure 4. A gate and delay generator (Ortec, Oak Ridge, TN, model 416A) is used to select the desired delay and width (duration) of the pulse of voltage to be delivered to the deflection EPG. The delay is set with respect to the start pulse and is monitored using a Tektronix (Beaverton, OR, model 475A) oscilloscope. When a start signal is received, the EPG voltage remains off for the set delay period and then is switched on for the duration of the pulse width. The pulse width is set to correspond to the time needed for the ions of interest to traverse the length of the EPG. The locations of the ions in time as they travel through the spectrometer can be determined using the ion trajectory program SIMION. SIMION can place time markers on ion trajectories to indicate the location of the ion as a function of time. Figure 5 shows time markers at every 1 μs for a singly charged bovine insulin molecular ion trajectory in the ^{252}Cf-PDMS spectrometer. Shown above the SIMION plot is a diagram of the waveform that would be selected on the basis of this simulation to collect a spectrum that would include the insulin molecular ion. The deflection voltage is turned on only after the ion of interest has passed through the entrance of the EPG and is turned off again before the ion reaches the EPG exit. In this way, the ion is not influenced by the fringe fields at the ends of the EPG, so its TOF is not perturbed from the value obtained without deflection voltage.

Sample Preparation

For these studies, targets were prepared by adsorbing sample from solution onto an electrosprayed matrix of either 9-anthroic acid [13] or purpurogallin on an aluminized Mylar film. The electrospraying procedure has been described elsewhere [14]. The matrix compound was dissolved in acetone to give a 1 μg/μL solution.

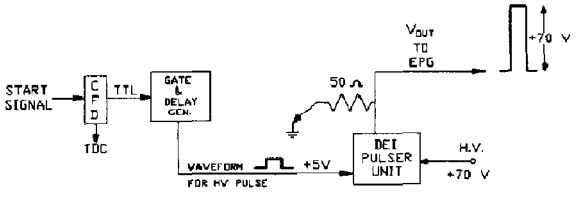

Figure 4. Block diagram of the deflection EPG pulser circuitry. TTL means transistor–transistor logic, referring to the pulse shape required by the gate and delay generator. CFD is the constant fraction discriminator and TDC is the time-to-digital converter.

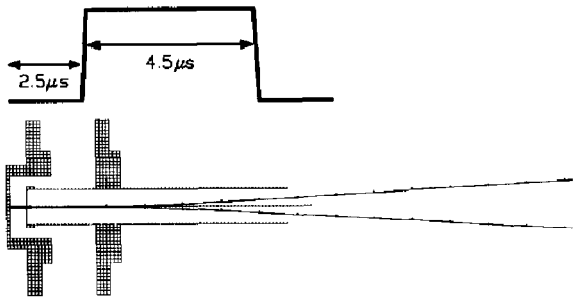

Figure 5. SIMION plot showing the molecular ion of bovine insulin traversing through the acceleration region and deflection EPG with +70 V on the inner conductor. Markings on the trajectories indicate 1-μs time intervals. Waveform above the plot shows the delay and width of the pulse that would be chosen on the basis of this plot.

A 200-μL volume was electrosprayed through a 6-mm diameter collimator onto the aluminized Mylar. The sample used as a model compound in these studies was bovine insulin (m/z 5734) obtained from Serva Biochemicals (Westbury, NY). The bovine insulin was dissolved in 0.1% aqueous trifluoroacetic acid to give a 1-mM solution. A 40-μL drop was spread over the surface of the 6-mm diameter matrix deposit and allowed to adsorb for 5 minutes. The target was then rinsed with 100 μL of high-purity water (Burdick and Jackson, Muskegon, MI) and spun at 10,000 rpm for 30 s with a photoresist spinner (Headway Research, Inc., Garland, TX) to remove solvent, impurities, and species that were not adsorbed.

Results and Discussion

Stop Detector

The initial testing of the new hybrid stop detector involved varying the voltage applied to the grid over the scintillator and measuring the peak intensities of the model protein spectrum obtained. The voltage applied affects the focusing and also the energy of the electrons that strike the scintillator. Thus this voltage affects both the intensity and the amplitude of the pulses obtained. The model protein used for this test was bovine insulin (m/z 5734). The insulin was adsorbed onto a 9-anthroic acid matrix for this experiment. Positive ions were accelerated to +15 kV and data were collected for 10-min acquisition periods at each different scintillator grid voltage. The results are shown in Figure 6 for (a) +3 kV, (b) +4 kV, and (c) +5 kV on the scintillator grid. The dramatic increase in the ratio of $[M + H]^+$ to $[M + 2H]^{2+}$ signals with increasing grid voltage indicates that increased amplitude of the $[M + H]^+$ signal is responsible for its increased peak height. The faster $[M + 2H]^{2+}$ ion produces more secondary electrons when it strikes the MCP and therefore gives higher amplitude signals than the $[M + H]^+$ ion does. At +4 kV on the scintillator grid, the pulse produced by the impact of the

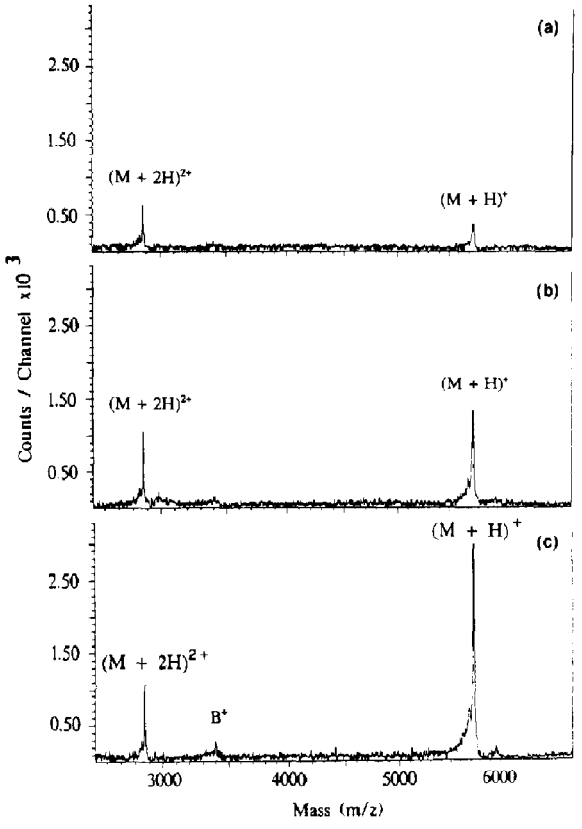

Figure 6. Molecular ion region of bovine insulin on a 9-anthroic acid matrix using the hybrid stop detector with (a) +3 kV, (b) +4 kV, and (c) +5 kV on the scintillator grid. (Counts/channel $\times 10^3$ on the y axis indicates that the value 2.50 corresponds to 2500.)

$[M + 2H]^{2+}$ ion already has an amplitude greater than the threshold level of the constant fraction discriminator (CFD). However, the impact of the slower $[M + H]^+$ ion on the MCP produces fewer electrons in the multiplication cascade so that the total energy deposited by the burst of these 4-keV electrons in the scintillator is not enough to produce a pulse with an amplitude greater than the constant fraction discriminator threshold. By increasing the electron energy to 5 keV (a scintillator grid voltage of +5 kV), the pulses produced by the $[M + H]^+$ ions are amplified to a level at which they trigger the CFD.

To compare the performance of the new hybrid stop detector to that of a conventional stop detector, identical samples were analyzed simultaneously in two different spectrometers. The spectrometer and conventional stop detector used for the comparison have been described by Mudgett [15]. The conventional detector consisted of an MCP chevron, focusing ring, and 50-ohm impedance-matched conical anode. The secondary ion flight path in this spectrometer was 53 cm in length. An Ortec model 9301 fast preamplifier (×10 amplification) was used with the conventional detector. The flight path used for the hybrid detector was 74 cm. The amplitude of the signal produced by the conventional stop detector for the hydrogen ion (H^+) was on the order of 800 mV after ×10 amplification by the preamplifier. No preamplifier was used with the hybrid detector because the gain was sufficiently large without it. The H^+ signal amplitude produced by the hybrid detector was approximately 1.5 V without the preamplifier. For this experiment the bovine insulin was adsorbed onto a purpurogallin substrate/matrix. Data were acquired for 10 min for each target in the two different spectrometers with +10 kV acceleration. The experiment was performed in duplicate in order to show reproducibility of the result. The results from the two experiments are shown in Table 1. The insulin molecular ion intensities were normalized to the intensity of H^+ in order to correct for differences in source strength and geometry between the two different spectrometers used. The H^+ ions produce large pulses in both the hybrid and conventional detector, such that the probability for detecting H^+ in each case is essentially 100%. In addition, the ratio of the insulin molecular intensity to H^+ ion intensity provides a relative measure of high mass sensitivity. Integrated intensities of the insulin $[M + H]^+$, $[M + 2H]^{2+}$, and H^+ peaks were used in calculating the normalized intensities shown in Table 1. This eliminated the differences in peak height due to the fact that the length of the field-free flight path was not the same for the two spectrometers. The results indicate that the hybrid detector does improve sensitivity for high mass detection by approximately 50% compared to the conventional chevron detector. For protein molecular ions of higher mass-to-charge ratio value than insulin, more dramatic improvements in sensitivity are expected with the use of higher scintillator grid voltages.

Optimization of Electrostatic Particle Guide Deflection Voltage

The EPG deflection voltage was optimized experimentally by determining the ion profiles for an actual sample in the spectrometer. The sample tested was bovine insulin adsorbed onto a 9-anthroic acid matrix. Positive ions were accelerated to +15 kV. Spectra were

Table 1. Spectral data for the molecular ion of bovine insulin on purpurogallin, with the conventional stop detector compared to the new hybrid stop detector[a]

	$[M + H]^+/H^+$	$[M + 2H]^{2+}/H^+$
Experiment 1		
Conventional	0.085	0.034
Hybrid	0.132	0.049
Experiment 2		
Conventional	0.075	0.029
Hybrid	0.124	0.054

[a] $[M + H]^+$ and $[M + 2H]^{2+}$ intensities are given as integrated intensities normalized to the H^+ integrated intensity for each spectrum.

recorded for EPG voltages from 0 V to 100 V in 10 V increments with the 38-mm barrier disk in place. The deflection voltage was constant (not pulsed) during each of the 5-min acquisitions. Integrated intensities of selected ion peaks were determined for each deflection voltage. For each ion, intensities were normalized to the intensity recorded for 0 V on the EPG. The resulting plots for H^+, the insulin molecular ion $[M + H]^+$, and the doubly charged insulin molecular ion $[M + 2H]^{2+}$ are shown in Figure 7. The error bars in these plots represent the statistical counting fluctuations (square root of the intensities) in the data. As shown in Figure 7a, the H^+ ion intensity reaches a maximum with a deflection voltage of +70 V. This voltage is consistent with the SIMION simulated ion trajectories (Figure 3), which predicted that a minimum of +70 V would be required for the ions to be deflected past the barrier disk.

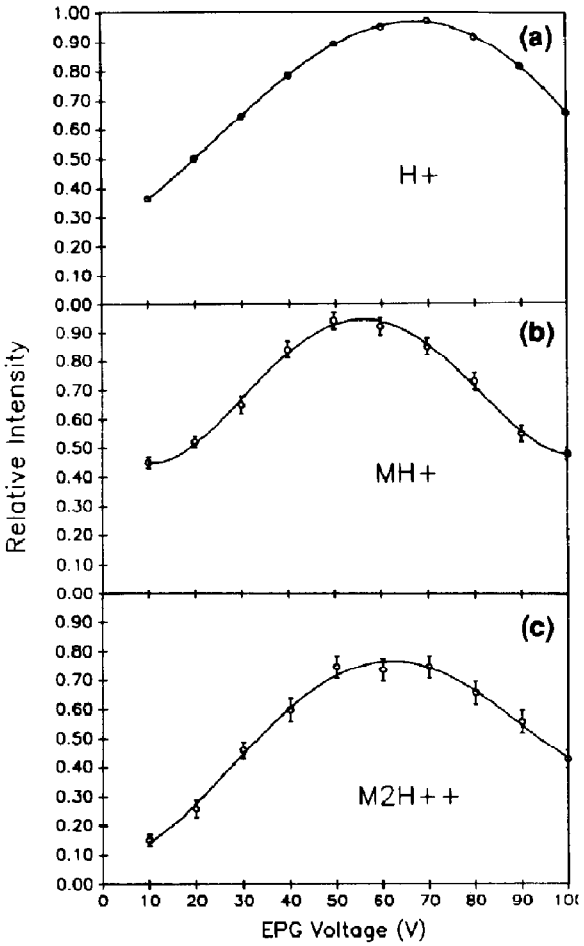

Figure 7. Plots of ion intensity from a bovine insulin sample for (a) H^+, (b) $[M + H]^+$, and (c) $[M + 2H]^{2+}$ ions as a function of EPG deflection voltage with the barrier disk in place. Intensities are normalized to the values obtained with 0 V on the deflection EPG and the barrier disk removed. The smooth curves represent a fit to the data.

For each of the three ions, intensities do not reach 100% of the values obtained with the EPG off (0 V) and the barrier disk removed. This loss is due in part to the elimination from the spectrum of neutral species that make a small contribution to the ion peaks. However, the major factor is the variation in the initial radial velocities associated with different ions when they are emitted from the target. Because of the variety of radial velocities within the ion beam, optimization of the EPG deflection voltage to deflect most ions beyond the barrier disk inevitably causes some ions to be deflected out of the area subtended by the MCP. Examination of the profiles in Figure 7 for the three ions reveals that the beam divergence differs for each ion type. At the minimum deflection voltage applied (+10 V), only 15% of the $[M + 2H]^{2+}$ ions are able to pass the barrier disk, whereas for H^+ and for $[M + H]^+$ the percentage of ions passing the disk are 37 and 45%, respectively.

Effect of Pulser Delay and Width

The initial pulser experiments with the deflection EPG and barrier disk were performed with an early version of the EPG, which had a thin (0.173-mm diameter) wire as the inner conductor. For this configuration, the optimum EPG deflection voltage was determined to be +200 V. The sample target used in this study was bovine insulin adsorbed onto a 9-anthroic acid substrate. An initial spectrum was recorded with the deflection EPG off and the barrier disk retracted. With the barrier disk in position and the EPG deflection voltage set at +200 V, spectra were acquired at various pulser settings. Acquisition times were 5 min for all spectra. Figure 8 compares the spectrum obtained with (a) no voltage on the deflection EPG (barrier disk out) to that obtained with (b) a deflection voltage of +200 V applied to the EPG (barrier disk in) by the pulser, having a delay of 3 μs and a width (duration) of 4 μs relative to the start signal. The background was reduced dramatically for the entire ^{252}Cf-PDMS spectrum when the pulsed deflection EPG was used. The delay and width of the pulse were selected in this case to deflect $[M + H]^+$ ions around the barrier disk optimally. Although some hydrogen ions were still detected (10%), most of the light ion intensity was eliminated. In addition, the $[M + 2H]^{2+}$ intensity was less, relative to the $[M + H]^+$ intensity, when the pulsed EPG was used. This is because of the 3-μs delay, which turns the deflection EPG on too late to deflect all of the $[M + 2H]^{2+}$ ions around the barrier disk. Only those $[M + 2H]^{2+}$ ions that traverse very close to the EPG inner conductor where the electric field gradient is highest receive enough deflection to bypass the barrier disk and are detected. The $[M + H]^+$ peak intensity was about 30% less when the pulsed deflection EPG was used, but the peak-to-background ratio increased from 4.1 to 9.1. As we will show, further

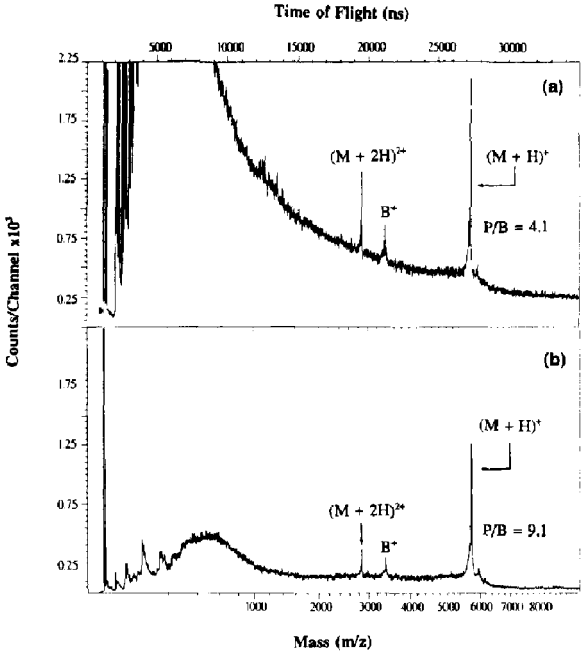

Figure 8. Complete ^{252}Cf-PDMS spectra of bovine insulin on a 9-anthroic acid substrate with (a) barrier disk out and no deflection EPG voltage and (b) barrier disk in and +200 V deflection voltage pulsed on with a 3-μs delay relative to the start signal and a 4-μs duration. (Counts/channel $\times 10^3$ on the y axis indicates that the value 2.25 corresponds to 2250.)

optimization of the pulsed EPG gave an additional improvement in peak-to-background ratio.

The effect of changing the delay of the deflection voltage pulse relative to the start pulse on the bovine insulin spectrum is shown in Figure 9. In each of the four spectra shown, the pulse width was set at 3 μs. This means that regardless of the delay, the EPG deflection voltage was on for a 3-μs period each time a start signal triggered the pulser. In Figure 9a the delay of the pulse was set at 2 μs. This means that 2 μs after the start signal triggers the pulser, the EPG deflection voltage is turned on. In Figure 9b, c, and d the delay was set at 3, 4, and 5 μs, respectively. As the delay was increased from 2 to 4 μs, the intensity of the $[M + 2H]^{2+}$ peak decreased and the $[M + H]^+$ intensity increased. When a 2-μs delay was used the $[M + H]^+$ ions did not receive as much deflection as the $[M + 2H]^{2+}$ ions, because the $[M + H]^+$ ions entered the EPG after the deflection voltage had already been switched on. Thus, the $[M + H]^+$ ions did not experience a radial force for the full 3 μs that the deflection voltage was applied to the EPG. When the 3-μs delay was used the situation was reversed, because the $[M + 2H]^{2+}$ ions exited the EPG before the 3-μs deflection period was over. At a delay of 4 μs the $[M + 2H]^{2+}$ peak has almost vanished and the B^+ fragment intensity also has begun to diminish. Finally, a delay of 5 μs did not provide enough deflection time even for the $[M + H]^+$ ions, decreasing that peak height and eliminating altogether the $[M + 2H]^{2+}$ and B^+ peaks from the spectrum.

Table 2 shows the peak heights (counts/channel at 16 ns/channel) and centroid TOF values and full width at half maximum (FWHM) values (both in nanoseconds) for the $[M + H]^+$ and $[M + 2H]^{2+}$ peaks from spectra taken at a variety of pulser settings. Also included in the table is the background level at the centroid of the $[M + H]^+$ peak and the peak-to-background ratio. The latter was calculated by first determining the intensity of the peak channel including the background. The background under the peak was subtracted by linear interpolation between the two channels at the beginning and end of the distribution. The background-subtracted peak intensity was then recalculated. This value divided by the number of subtracted background counts is defined as the peak-to-background ratio.

The first column in Table 2 gives values for a spectrum taken without the pulsed deflection EPG (barrier disk retracted). The rest of the columns give the data for the deflection EPG pulsed on (barrier disk in place) with a voltage of +200 V, and various pulse delays and widths as shown. The direct result of increasing the pulse width for a given delay is that the deflection voltage remains on for a longer period. This means that the ions traversing through the EPG during the time that the EPG is pulsed on will receive a greater deflection when the pulse width is increased. This effect is illustrated in Table 2. For a given delay, the longer deflection periods enable more ions of interest to be deflected past the barrier disk (i.e., ion intensities increase).

The study of the effects of the pulser delay and width settings on bovine insulin spectra also serves to illustrate fringe field effects. When a 2-μs delay is used the deflection voltage is turned on after the $[M + 2H]^{2+}$ ion has entered the EPG but before the $[M + H]^+$ ion has entered. This means that the $[M + H]^+$ ion is influenced by the fringe fields at the EPG entrance, but the $[M + 2H]^{2+}$ ion is not. This effect is supported by the data in the first few columns of Table 2, which show that the $[M + H]^+$ peak is perturbed to a longer TOF while the $[M + 2H]^{2+}$ TOF remains about the same. At a pulse width of 4 μs (delay 2 μs), the $[M + 2H]^{2+}$ TOF begins to show centroid shifts due to the fringe fields at the exit of the EPG, resulting in a decrease in the centroid TOF. The $[M + H]^+$ ion is affected by both the entrance and exit fringe fields for pulse widths of 5 and 8 μs (delay 2 μs). In this situation the acceleration at the exit begins to compensate for the deceleration at the entrance, so that the centroid TOF decreases but remains higher than the TOF observed without the deflection EPG. The large FWHM values for $[M + H]^+$ when the 2-μs delay is used are also indicative of the significant perturbation that is taking place. A 3-μs delay is sufficient to allow the $[M + H]^+$ ion to enter the EPG before the deflection voltage is applied. With this delay setting, a pulse

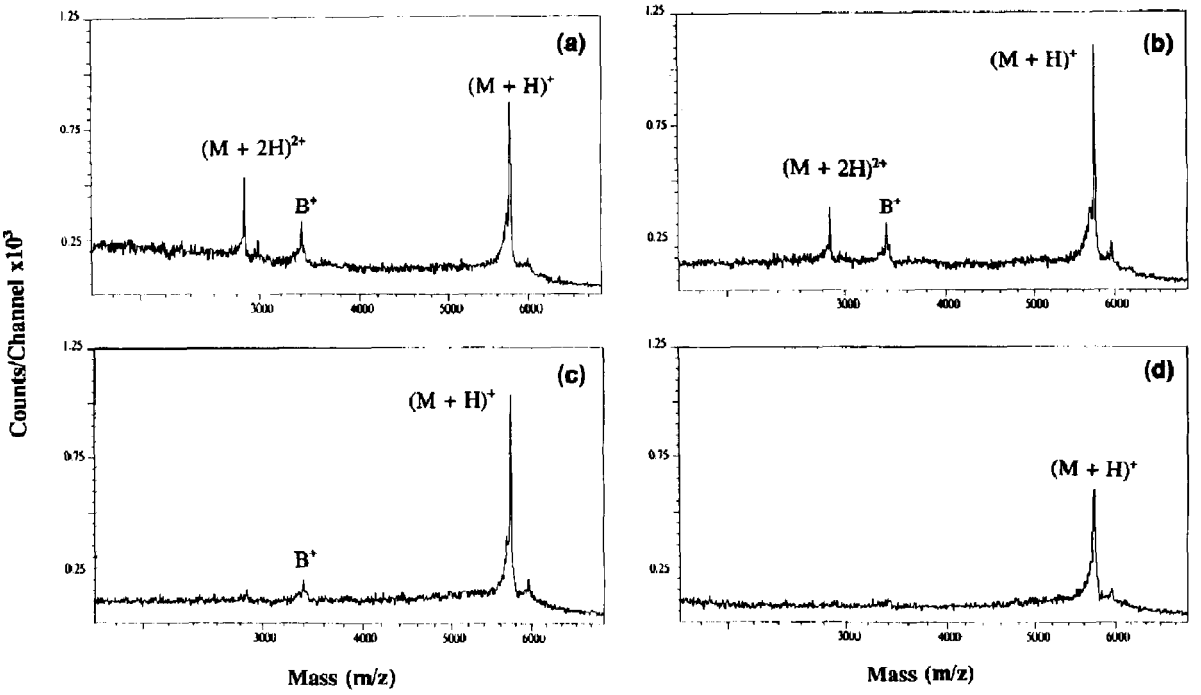

Figure 9. Effect of deflection EPG pulse delay on the molecular ion region of bovine insulin spectra. The pulse width in each case is 3 μs. The pulse delay is (a) 2 μs, (b) 3 μs, (c) 4 μs, and (d) 5 μs. Acquisition times were 5 min. (Counts/channel $\times 10^3$ on the y axis indicates that the value 1.25 corresponds to 1250.)

width of up to 4 μs ensures that the deflection voltage is turned off before the $[M + H]^+$ ion exits the EPG. In this way, the $[M + H]^+$ ion escapes the effects of the fringe fields altogether and the resulting centroid TOF is quite close to that observed in the spectrum taken without the deflection EPG. At a pulse width of 7 μs (3-μs delay), the $[M + H]^+$ ion is accelerated by the exit fringe fields and the centroid TOF is shortened. The same effect is achieved with longer delays, as shown in the last two columns of the table. For the 3-μs delay and 2–4 μs-width pulses, the FWHM values are closer to the undeflected values, but at best remain 25% higher. We suspected that the thin wire being used as the inner conductor on the EPG was not rigid enough to achieve the straight field lines necessary to prevent any TOF perturbation. To eliminate this problem, we replaced the wire with a stiff self-supporting 1.6-mm-diameter stainless steel rod.

The replacement of the fine wire with the stainless steel rod reduced the FWHM values obtained when

Table 2. Spectral data for bovine insulin molecular ions as a function of the deflection EPG pulser delay and width

EPG (V)	0	200	200	200	200	200	200	200	200	200	200	200
Delay (μs)	none	2	2	2	2	2	3	3	3	3	4	5
Width (μs)	none	2	3	4	5	8	2	3	4	7	3	3
$[M + H]^+$												
Peak height[a]	1,620	490	717	959	866	882	930	951	1,142	929	905	512
TOF[b]	27,271	27,324	27,320	27,326	27,306	27,297	27,273	27,276	27,271	27,259	27,262	27,242
FWHM	36	56	60	67	67	57	49	47	45	47	60	74
Background[c]	394	110	133	138	125	129	116	124	125	131	116	95
P/B[d]	4.1	4.5	5.4	7.0	6.9	6.8	8.0	7.7	9.1	7.1	7.8	5.4
$[M + 2H]^{2+}$												
Peak height	670	312	351	382	342	359	230	249	260	220	73	0
TOF	19,520	19,524	19,523	19,513	19,505	19,511	19,492	19,498	19,499	19,496	19,498	N/A
FWHM	25	49	47	38	33	47	43	42	40	44	N/A	N/A

[a] Peak heights are given in counts per channel, 16 ns/channel spectra.
[b] TOF and FWHM are given in nanoseconds, 1 ns/channel spectra.
[c] Background levels determined at the $[M + H]^+$ centroid, 16 ns/channel spectra.
[d] Peak/background calculated from the $[M + H]^+$ peak height and background values.

the pulsed deflection EPG was used. A comparison of $[M + H]^+$ data for spectra taken without deflection to spectra taken with the pulsed deflection EPG is shown in Table 3 for bovine insulin on two different substrates. Both targets were analyzed with +15 kV acceleration, but the acceleration distance was 6 mm for the purpurogallin and 8 mm for the 9-anthroic acid substrate. Acquisition times were 5 min. The optimum pulser settings for the new EPG were determined to be a 2-μs delay, a 2.5-μs width, and a +100-V deflection voltage. This delay and width ensured that the trajectory of the $[M + H]^+$ ion was not perturbed by fringe fields. As shown in Table 3, the FWHM values for $[M + H]^+$ did not increase when pulsed deflection was applied using the new EPG. We attribute this improvement to the more uniform equipotential field lines obtained when the rigid rod is used instead of the thin wire.

Background Reduction

The data in Table 3 represent the optimum background reduction conditions for improving peak-to-background ratios with the pulsed deflection EPG. As shown in Table 3, an increase of almost 300% in peak-to-background values was obtained for both targets when the pulsed deflection EPG was used. The insulin–purpurogallin target gave a much higher deflected $[M + H]^+$ peak height relative to the nondeflected peak height than did the insulin–9-anthroic acid target. This is probably due to the deposit size, which was larger (9-mm diameter) for the insulin–purpurogallin target. The insulin–9-anthroic acid target diameter was 6 mm. The ions desorbed from the purpurogallin substrate probably had a greater beam diameter, resulting in improved ion collection for the deflection EPG mode. The background reduction and improvement in peak-to-background for the insulin–purpurogallin target is shown graphically in Figure 10. Figure 10a gives the molecular ion region of a spectrum recorded without the deflection EPG (barrier disk retracted) and Figure 10b shows the same region of a spectrum recorded with the pulsed deflection EPG (+100 V, 2-μs delay, and 2.5-μs width). When the pulsed deflection was used, a 65% background reduction with minimal loss of peak intensity improved the quality of the spectrum, allowing the B^+ fragment (corresponding to the B-chain of the insulin molecule) to be seen more clearly. Finally, the insulin–9-anthroic acid target gave much more spectacular peak-to-background values than did the insulin–purpurogallin target. The peak-to-background value of 29/1 was by far the best value ever recorded by ^{252}Cf-PDMS for an ion above mass 5000 u. This spectrum is shown in Figure 11.

Table 3. Spectral data for the molecular ion of bovine insulin on two different substrates, with and without the pulsed deflection EPG

EPG (V)	0	100
Delay (μs)	none	2.0
Width (μs)	none	2.5
$[M + H]^+$ data for bovine insulin–purpurogallin		
Peak height[a]	750	708
TOF[b]	27,311	27,309
FWHM	44	43
Background[c]	207	74
P/B[d]	3.6	9.6
$[M + H]^+$ data for bovine insulin–9-anthroic acid		
Peak height	1,347	755
TOF	27,441	27,439
FWHM	36	35
Background	134	26
P/B	10	29

[a] Peak heights are given in counts per channel, 16 ns/channel spectra.
[b] TOF and FWHM are given in nanoseconds, 1 ns/channel spectra.
[c] Background levels determined at the $[M + H]^+$ centroid, 16 ns/channel spectra.
[d] Peak/background calculated from the $[M + H]^+$ peak height and background values.

Nonselected Light Ions in the Pulsed Electrostatic Particle Guide Spectrum

In Figure 11 a broad distribution appears in the spectrum at m/z 800–2000. The appearance of this distribution is characteristic of spectra recorded using the

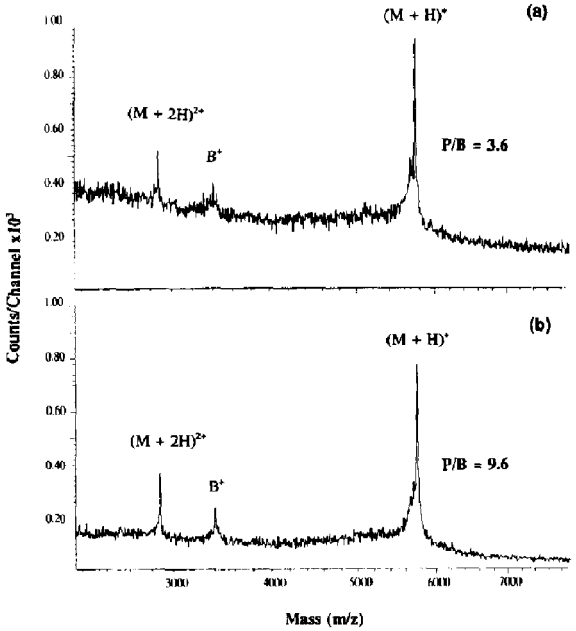

Figure 10. Molecular ion region of a spectrum of bovine insulin adsorbed onto a purpurogallin substrate. The undeflected spectrum is shown in (a). The pulsed deflected spectrum using the EPG with the 1.6-mm diameter inner conductor (2-μs delay, 2.5-μs width, +100 V) is shown in (b). (Counts/channel × 10^3 on the y axis indicates that the value 1.00 corresponds to 1000.)

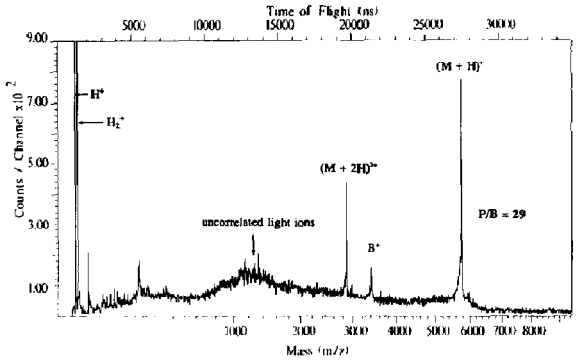

Figure 11. Entire ^{252}Cf-PDMS spectrum of bovine insulin adsorbed onto a 9-anthroic acid substrate using the pulsed deflection EPG with the 1.6-mm diameter inner conductor, with a pulse delay of 2 μs, a width of 2.5 μs, and +100 V deflection. (Counts/channel $\times 10^2$ on the y axis indicates that the value 9.00 corresponds to 900.)

pulsed deflection EPG. Another example was shown in Figure 8, wherein the distribution appeared in the mass range m/z 500–1000, but the EPG used (thin wire inner conductor) had slightly different dimensions. From the pulse width and delay studies we observed that the location of this distribution of ions in the spectrum varied directly as a function of the pulse width and delay. From this we deduce that the distribution consists of two components. One component is comprised of correlated ions that miss the neutral particle barrier when the deflection EPG voltage is zero. These ions produce sharp peaks. Superimposed on these peaks is a smooth background of uncorrelated light ions that are in the EPG when the deflection voltage is turned on. In the case shown in Figure 11, the pulse has been set up to deflect the molecular ions of insulin. The light ions that are located within the deflection EPG when it is switched on cannot be correlated with the event that desorbed the molecular ions of insulin. These uncorrelated ions are nevertheless deflected around the barrier disk and detected. They appear as an unresolved background in the spectrum because the ions have a distribution of masses and hence velocities, and their formation is not correlated with a valid start pulse. Also appearing in the spectrum are the H^+ and H_2^+ ions, as well as a few other light ions (below m/z 500). These ions are observed in the spectrum because they have a large radial velocity component so that some are able to pass by the barrier disk even without voltage on the deflection EPG. Most of the light ions emitted (95%) are stopped by the barrier disk, so the intensities of these peaks are greatly reduced compared to a spectrum taken with the barrier disk retracted.

Conclusion

In future studies the use of the pulsed deflection EPG to enhance peak-to-background ratios will improve the detection limit of ^{252}Cf-PDMS for higher molecular weight ions. Furthermore, peptide and protein sequencing by the analysis of fragmentation patterns in ^{252}Cf-PDMS [16] will benefit from the pulsed deflection EPG. The yield of individual fragment ions in ^{252}Cf-PDMS is typically small relative to the molecular ion yield. By bracketing a specific region of the spectrum using the pulsed deflection EPG, the sensitivity for detection of fragment ion peaks within the selected region will be improved. Finally, the pulsed deflection EPG system could be used for detection of an ion of unknown molecular weight. Usually the researcher knows or suspects that the molecular weight of an unknown ion is within a certain mass range. When the ion is unknown, the mass spectrometrist can simply bracket a relatively large deflection time window in the region of the suspected molecular weight.

Acknowledgments

We thank Dennis Shelton for technological contributions to this project. This research was sponsored by the National Institutes of Health (GM-26096) and the Robert A. Welch Foundation (A-258).

References

1. Macfarlane, R. D.; Sundqvist, B. U. R. *Mass Spectrom. Rev.* **1985**, *4*, 421–460.
2. Jonsson, G.; Hedin, A.; Hakansson, P.; Sundqvist, B.; Bennich, H.; Roepstorff, P. *Rapid Commun. Mass Spectrom.* **1989**, *3*, 190–191.
3. McNeal, C. J.; Hughes, J. M.; Lewis, G. J.; Dahl, L. F. *J. Am. Chem. Soc.* **1991**, *113*, 372–373.
4. Karas, M.; Ingendoh, A.; Bahr, U.; Hillenkamp, F. *Biomed. Environ. Mass Spectrom.* **1989**, *18*, 841–843.
5. Smith, R. D.; Loo, J. A.; Edmonds, C. G.; Barinaga, C. J.; Udseth, H. R. *Anal. Chem.* **1990**, *62*, 882–899.
6. Sundqvist, B.; Kamensky, I.; Hakansson, P.; Kjellberg, J.; Salehpour, M.; Widdiyasekera, S.; Fohlman, J.; Peterson, P.; Roepstorff, P. *Biomed. Mass Spectrom.* **1984**, *11*, 242–257.
7. Hedin, A.; Hakansson, P.; Sundqvist, B. *Int. J. Mass Spectrom. Ion Proc.* **1986**, *70*, 203–212.
8. Wolf, B.; Mudgett, P. D.; Macfarlane, R. D. *J. Am. Soc. Mass Spectrom.* **1990**, *1*, 28–36.
9. Oakey, N. S.; Macfarlane, R. D. *Nucl. Instrum. Methods* **1967**, *49*, 220–228.
10. Dahl, D. A.; Delmore, J. E. SIMION, version 4.0; EGG-CS-7233; EG&G Idaho, Idaho National Engineering Laboratory, Idaho Falls, ID, 1988.
11. Geno, P. W.; Macfarlane, R. D. *Int. J. Mass Spectrom. Ion Phys.* **1986**, *74*, 43–57.
12. Macfarlane, R. D.; Hill, J. C.; Jacobs, D. L. *J. Trace Microprobe Tech.* **1986–87**, *4*, 281–302.
13. Wolf, B.; Macfarlane, R. D. *J. Am. Soc. Mass Spectrom.* **1991**, *2*, 29–32.
14. McNeal, C. J.; Macfarlane, R. D.; Thurston, E. L. *Anal. Chem.* **1979**, *51*, 2036–2039.
15. Mudgett, P. D.; Ph.D. Dissertation, Texas A&M University, 1991.
16. Bunk, D. M.; Macfarlane, R. D. *J. Am. Soc. Mass Spectrom.* **1991**, *2*, 379–386.